Structural Models of the Photointermediates in the Rhodopsin Photocascade, Lumirhodopsin, Metarhodopsin I, and Metarhodopsin II

Masaji Ishiguro,*[a] Yoshiaki Oyama,[b] and Takahiro Hirano[a]

Model building of the two photointermediates, lumirhodopsin and metarhodopsin I, and the activated form of rhodopsin, metarhodopsin II, is described. An outward swing of the C-terminal portion of transmembrane segment 3, pivoting on Cys110 at the N-terminal end of transmembrane segment 3, led to structural models of lumirhodopsin and metarhodopsin I. The conformation of the chromophore in the lumirhodopsin and metarhodopsin I models is controlled by the motion of transmembrane segment 3 and agreed closely with the hydrogen-bonding states of the protonated Schiff base in lumirhodopsin and metarhodopsin I as deduced from their FTIR and resonance Raman spectra and with the negative and positive CD bands of lumirhodopsin and metarhodopsin I, respectively. The structure of metarhodopsin II was constructed by an outward swing of transmembrane segment 3 and the rigid-body motion of transmembrane segment 6. The arrangement of the entire transmembrane segment of the metarhodopsin II model closely agreed with the electron paramagnetic resonance spectra of spin-labeled rhodopsin mutants and provided a structural basis for the protonation of Glu134, which is a key process in transducin activation.

Introduction

Seven-helix integral membrane proteins, G-protein-coupled receptors (GPCRs), constitute a major family of transmembrane receptors that mediate the transduction of extracellular signals to the inside of cells. The binding of agonists to the GPCR structurally changes the protein, a change which is recognized by heterotrimeric G proteins at an intracellular site. Rhodopsin is an inactive form of a GPCR that forms a protonated Schiff base (PSB) with the inverse agonist, 11-*cis*-retinal, at Lys296 of opsin, a seven-helix integral membrane protein. Rhodopsin can be photochemically converted into the activated form, metarhodopsin II, by isomerization of the 11-*cis*-retinylidene chromophore to the all-*trans* chromophore, a full agonist.[1, 2]

Light causes an extremely rapid 11-*cis* to all-*trans* isomerization of the chromophore.[1] The following bleaching intermediates are observed along the photoactivation cascade. An early photointermediate, bathorhodopsin, which already contains a photoisomerized all-*trans*-retinylidene chromophore, slowly decays with conformational changes to metarhodopsin I via lumirhodopsin within approximately 1 μs. Deprotonation of the Schiff base in the following thermal decay of metarhodopsin I yields metarhodopsin II, which activates the G protein, transducin.[2, 3]

The *cis*–*trans* photoisomerization of the chromophore occurs within the limited space of opsin and affords a highly strained conformation of the chromophore.[4] The protein moiety increases in volume in the formation of lumirhodopsin at physiological temperatures.[5, 6] The flip of the modified β-ionone moiety suggests that transmembrane segments (TM) 3 and 4 rearrange to accommodate the modified β-ionone moiety[7] and the increase in volume may thus be attributed to the rearrangement of TM3 and TM4.

Data from FTIR and NMR spectra show that the chromophore in the lumirhodopsin and metarhodopsin I states assumes a relaxed form relative to the more constrained all-*trans* conformation in bathorhodopsin.[8, 9] CD measurements have shown that the chromophore in lumirhodopsin appears as a negative band whereas that in metarhodopsin I is characterized by a positive band;[10, 11] this indicates that the transition from lumirhodopsin to metarhodopsin I includes a characteristic conformational change of the polyene moiety of the chromophore. Time-resolved resonance Raman spectroscopy measurements of the chromophore structure in lumirhodopsin and metarhodopsin I have revealed that the PSB hydrogen bonding is significantly weakened during the bathorhodopsin to lumirhodopsin transition, whereas normal hydrogen bonding is recovered during the lumirhodopsin to metarhodopsin I transition.[12] This indicates that the conformational change of the polyene portion of the chromophore in the lumirhodopsin to metarhodopsin I transition is coupled with the conformational change of the PSB region.

A twisted C11−C12 double bond in bathorhodopsin might cause the cyclohexenyl group to flip towards TM3 and the concomitant rearrangement of TM3 and TM4 in the bathorhodopsin to lumirhodopsin transition.[7, 13] The rearrangement of TM3 and TM4 in the ground state was also suggested by a

[a] *Dr. M. Ishiguro, Dr. T. Hirano*
Suntory Institute for Bioorganic Research
1–1 Wakayamadai, Shimamoto, Osaka 618-8503 (Japan)
Fax: (+81) 75-962-2115
E-mail: ishiguro@sunbor.or.jp

[b] *Y. Oyama*
Daiichi-Suntory Ltd., Biomedical Research Institute
1–1 Wakayamadai, Shimamoto, Osaka 618-8503 (Japan)

  DOI: 10.1002/cbic.200300668

modeling study of rhodopsin analogues binding bulkier chromophores such as retinal analogues with a 5-membered fused ring.[14]

We previously described a model of bathorhodopsin that suggests a flip of the cyclohexenyl group towards TM3 and TM4, from which a subsequent photointermediate model could be generated.[13] Here, we describe a model-building study on the protein moiety of lumirhodopsin and metarhodopsin I through alteration of the arrangement of TM3 and TM4. We also performed a restrained molecular dynamics study on the conformational change of the chromophore of each altered protein structure in the bathorhodopsin to metarhodopsin I transition. We obtained conformationally different structures of the chromophore for lumirhodopsin and metarhodopsin I, in which the PSB showed distinct hydrogen-bond states with the counterion, Glu113, and the polyene portion showed opposite twist modes.

Photoaffinity-labeling experiments indicated that a modified β-ionone flips towards TM4 in the formation of lumirhodopsin and that the flipped conformation is maintained throughout the lumirhodopsin to metarhodopsin II transition.[7] EPR measurements of spin-labeled rhodopsin (in the dark) and metarhodopsin II (in the light) suggested that the rigid-body rotation of TM6 is involved in the generation of the metarhodopsin II state.[15] The importance of the motion of TM6 in the activation of rhodopsin has also been demonstrated by zinc cross linking of histidines.[16] Furthermore, the motion of TM6 is similar in other GPCRs such as the β2-adrenergic receptor.[17]

Formation of the metarhodopsin II state requires PSB deprotonation.[18] Neutralization of the PSB renders TM3 mobile enough to leave TM7. Concomitantly, an important proton-transfer process is required at the intracellular site for the activation of transducin, the G protein.[19] The highly conserved Glu134 appears to be responsible for the protonation by transferring the carboxylic acid side chain from a polar to a nonpolar environment,[20] although the mechanism of the structural change during this process is obscure. Thus, the aim of the present study of metarhodopsin II was the investigation of the structural origin of the rigid-body motion of TM6 and of the protonation of the particular residue at the intracellular site. Since crystallizing the unstable photointermediates is not possible and the computational simulation of all the photochemical transition from rhodopsin to metarhodopsin II (≈ms timescale) is beyond computational ability, another approach was required to produce models of metarhodopsin II. A model of metarhodopsin II has been constructed by using interhelical distances estimated from EPR measurements and from disulfide formation experiments.[21] However, elucidating the roles of the conserved residues and the process of photointermediate formation remains difficult. The photoconversion process is dependent on two temperatures during the lumirhodopsin to metarhodopsin II transition. At physiological temperatures, lumirhodopsin rapidly equilibrates with metarhodopsin I_{380}, a reaction followed by the formation of metarhodopsin II.[22] The chromophore of metarhodopsin I_{380} has a neutralized Schiff base, as indicated by its UV absorption maximum at 380 nm. This suggests that metarhodopsin I_{380} has a more mobile TM3 than metarhodopsin I, although whether metarhodopsin I_{380} binds or activates transducin remains unknown. In the photoconversion process at low temperatures, metarhodopsin I is a stable intermediate in the lumirhodopsin to metarhodopsin II transition. The chromophore of metarhodopsin I retains the PSB and the protein moiety does not bind transducin. Time-resolved UV measurements detected another intermediate, metarhodopsin Ib, in the transition of chicken metarhodopsin I to metarhodopsin II.[23] Since then, metarhodopsin Ib has been detected in the metarhodopsin I to metarhodopsin II transition of the bovine rhodopsin photocascade.[24] This photointermediate binds, but does not activate, transducin. This suggests that an inactive form of transducin binds before the formation of metarhodopsin II. The structural modeling of metarhodopsin II described here included the photochemical process at physiological temperatures, from a lumirhodopsin model through a metarhodopsin I_{380} model, with the assumption that the helix-forming hydrogen bond in each transmembrane helix is maintained during changes in their arrangement.

The present model-building studies of the early photointermediates, lumirhodopsin and metarhodopsin I, showed that the conformations of the chromophore closely agreed with the observed spectral data, such as UV, FTIR, and laser Raman spectra. Model building of the final active form of rhodopsin, metarhodopsin II, suggested that the highly conserved residues on TM3 – 7 play important roles during the structural change and the activation of transducin.

Results and Discussion

The crystal structure of rhodopsin[25–27] affords the basis for a glimpse of the isomerization of the chromophore and opsin through modeling of the photointermediates. The photochemical isomerization of the retinylidene chromophore is accompanied by a structural change of the protein moiety.[7] Molecular dynamics calculations have suggested that the hula-twist isomerization[28] at the C11—C13 portion generates the twisted C11—C12 double bond together with twisted C10—C11 and C12—C13 bonds for the initial isomerization during the rhodopsin to bathorhodopsin transition, while the PSB is unchanged.[13] The twisted high-energy conformation in bathorhodopsin[4] suggested that outward motion of TM3 is required to accommodate the relaxed conformation of the cyclohexenyl moiety in the following state.[13] We built models of lumirhodopsin and metarhodopsin I based on the following assumptions. 1) The N-terminal end of TM3 is anchored to the second extracellular loop by forming a highly conserved disulfide bond between Cys110 and Cys187. Thus, the C-terminal end of TM3 would swing outward, by pivoting at the highly conserved Cys110 residue. 2) The three-helix bundle of TM1, TM2, and TM7 would remain unchanged through the hydrogen-bond network formed by the highly conserved Asn55 on TM1, Asp83 on TM2, and Asn302 on TM7 at the protein interior as well as the hydrogen bond between Asn73 on TM2 and Tyr306 on TM7 at the intracellular site. 3) Thus, TM3 would swing towards TM4 to avoid collision with TM2. 4) The steric interactions between TM3

and TM4 would be properly removed by structural minimization without any constraints on the TM4 region (Asn151 – Trp175).

Although the motion of the C-terminal end of TM3 within 1.0 Å did not provoke a significant deformation of the helical structure of TM4 in the structure minimization of the N-terminal end of TM4, the C-terminal end of TM3 was swung every 0.2 Å while building models of lumirhodopsin and metarhodopsin I. The minimized structures of TM4 indicated a swing of TM4, by pivoting at Pro171. The conformation of the retinylidene chromophore in each minimized structure of the protein moiety was optimized by the molecular dynamics calculation and we selected the model structures of lumirhodopsin and metarhodopsin I that account for the spectral data (laser Raman, FTIR, and CD spectra) observed for their chromophore.

Structural model of lumirhodopsin

TM3 was swung until the double bonds of the polyene portion became a relaxed all-*trans* form from the C11—C12 twisted double bond of the chromophore of the bathorhodopsin model. Thus, the C-terminal end of TM3 was moved by about 1 Å and the concomitant structure minimization of TM4 yielded a swing of the N-terminal end of TM4 of about 2 Å (Figure 1). The

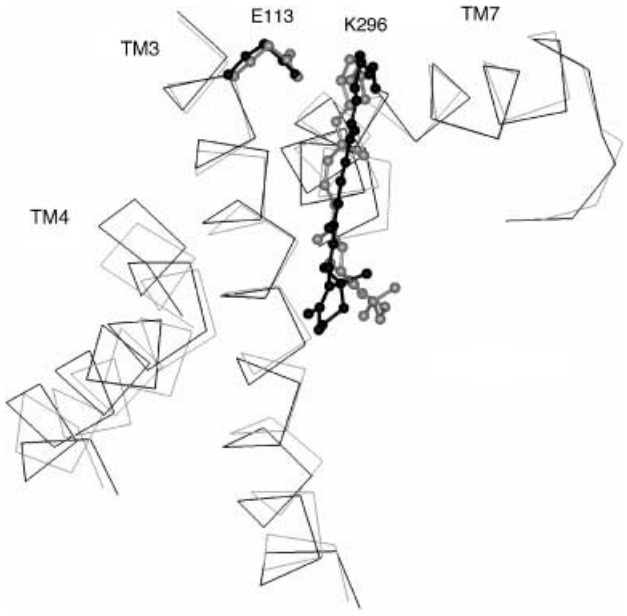

Figure 1. *Motion of TM3 and TM4 in the lumirhodopsin model (viewed from the extracellular site). Cα traces for TM3, TM4, and TM7, the chromophore, and two residues (E113 and K296) of lumirhodopsin are shown in black. The corresponding structures of the rhodopsin crystal are shown in gray. The one letter code is used for amino acid residues.*

rearrangement of TM3 and 4 provided a space for the cyclohexenyl moiety to flip towards TM3 and TM4. The flip of the cyclohexenyl group resulted in about a 40° rotation of the 9-methyl group about the axis of the C9—Nζ portion from the chromophore structure in rhodopsin. This rotation was predicted from the twist of the C11—C12 double bond (32°) in the bathorhodopsin model.[13] Concomitantly, the PSB proton (Hζ) rotated out of the hydrogen-bond-forming distance (3.1 Å for Hζ—Oε) and the polyene portion of the model lined up perpendicularly to the putative membrane plane, thereby directing the 9- and 13-methyl groups towards the extracellular site (Figure 2). The dislocation of the PSB proton is consistent

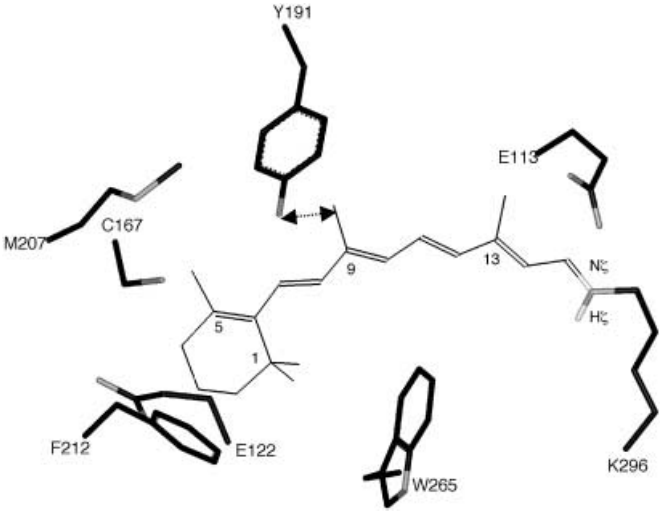

Figure 2. *Conformation of the chromophore in the lumirhodopsin model (lateral view; the extracellular site is at the top). Selected residues neighboring the chromophore are shown by black sticks and heteroatoms (N and O) are shown by gray sticks. Hydrogen atoms except for the PSB proton (Hζ) are neglected for clarity.*

with the disappearance of the hydrogen-bond acceptor for the PSB proton in lumirhodopsin.[12, 29] Although the carboxylate oxygen atom of Glu113 did not form a hydrogen bond with the PSB proton, it is located close to the PSB nitrogen atom (3.3 Å) and its negative charge would thus contribute to the localization of the cationic charge on the PSB nitrogen atom. A steric interaction between the phenolic oxygen atom of Tyr191 and the 9-methyl group of the chromophore appears to confine the polyene plane perpendicular to the membrane plane. The polyene plane showed a slight but significant left-twisted conformation with negative twists at the single bonds of C6—C7 through to C14—C15 (−167°, −177°, −180°, −173°, and −174°, respectively). The right or left twist of the polyene moiety has been correlated with positive or negative CD bands observed in rhodopsin and bathorhodopsin, respectively, by computational modeling and ab initio quantum chemical calculations.[13, 30, 31] In this sense, the negative twist of the polyene moiety of the lumirhodopsin model is consistent with the negative CD band observed for lumirhodopsin.[10] Molecular dynamics calculations suggest that the flip of the cyclohexenyl moiety accompanies the rotation of the C6—C7 bond from an *s-cis* to *s-trans* bond. In this conformation, the *gem*-dimethyl group at C1 pointed towards Trp265. Although it is not evident whether the C6—C7 bond assumes an *s-cis* or *s-trans* conformation in lumirhodopsin and rotation of the cyclohexenyl ring would not be important for transducin activation,[32] cyclohexenyl-ring rotation might contribute to the decay of

bathorhodopsin as discussed in 5-demethyl and mesityl analogues of rhodopsin.[33]

Structural model of metarhodopsin I and comparison with the lumirhodopsin model

Lumirhodopsin is more favorable than metarhodopsin I in the dry state.[34] This suggests that metarhodopsin I has more space for introducing water molecules, which stabilize the metarhodopsin I state. Since the extracellular surface would not change until metarhodopsin II is formed, water molecules would penetrate only from the intracellular site. Hence, we assumed that a further outward swing of the C-terminal portion of TM3 yields an open space for water molecules as well as for a more relaxed structure of the chromophore and we established the following criteria for assigning the conformation of the chromophore of metarhodopsin I. The PSB should recover a normal hydrogen bond from a considerably weakened hydrogen bond in lumirhodopsin as determined from the laser Raman spectra of metarhodopsin I[12] and the conformation should be consistent with the CD band signal opposite to that of lumirhodopsin.[10, 11]

A further swing of the C-terminal end of TM3 by 2 Å and a concomitant swing of the N-terminal end of TM4 by 4 Å led to a significant conformational change of the chromophore. The outward motion of TM3 removed the steric interaction between Tyr191 and the 9-methyl group in the lumirhodopsin model, thereby enabling the 9-methyl group to rotate beyond the Tyr191 residue. The chromophore rotated about 90° from that of the lumirhodopsin model and thus the polyene plane lay parallel to the putative membrane plane, as shown in Figure 3. The rotation of the chromophore reoriented the PSB proton (Hζ) to within hydrogen-bond-forming distance (2.3 Å) of the carboxylate oxygen atom and induced a conformational change of the Trp265 residue that was mainly due to steric interaction with the 13-methyl group. The flip of the cyclohexenyl group provided space for the conformational change of Trp265. Then, the polyene plane lay on the indole group of Trp265 and the 9-methyl group became proximal to Trp265. A Trp265Phe mutant and 9-demethyl retinal-bound rhodopsin become stable at the metarhodopsin I state,[35, 36] a fact suggesting that interaction between the 9-methyl group and Trp265 would destabilize the metarhodopsin I state. The cyclohexenyl moiety was proximal to Cys167 on TM4 and interrupted the hydrogen bond between His211 on TM5 and Trp126 on TM3. Thus, the hydrogen bond of His211 with Trp126 would weaken, while Glu122 was located within hydrogen-bond-forming distance of Trp126. This would coincide with the tightly hydrogen-bonded carbonyl group of Glu122 observed by FTIR spectra at the metarhodopsin I state.[37] A space generated by the flip of the chromophore was compensated for by the conformational change of the aromatic side chains of Phe208 and Phe212 on TM5, in addition to Trp265. The overall structure of the chromophore showed a right-twisted conformation with positive dihedral angles of 165°, 174°, 175°, 179°, and 171° for the single bonds of C6—C7 through to C14—C15. The mode of the twist is opposite to that of lumirhodopsin, as shown in Figure 4,

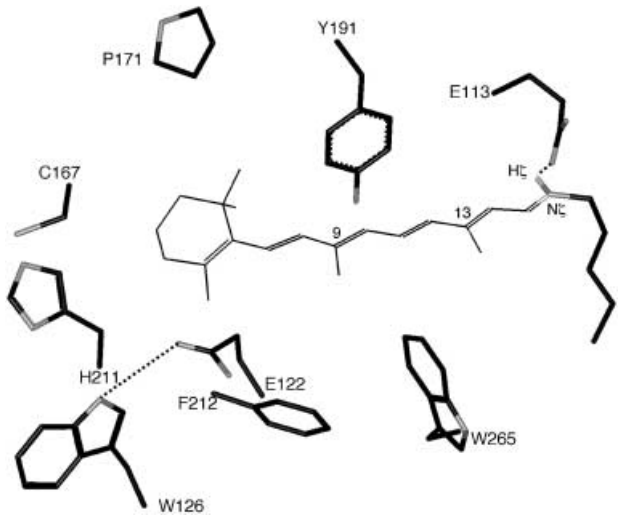

Figure 3. Conformation of the chromophore in the metarhodopsin I model (view from the extracellular site). Selected residues neighboring the chromophore are shown by stick models. Dotted lines indicate hydrogen bonds. Hydrogen atoms except for the PSB proton (Hζ) are neglected for clarity.

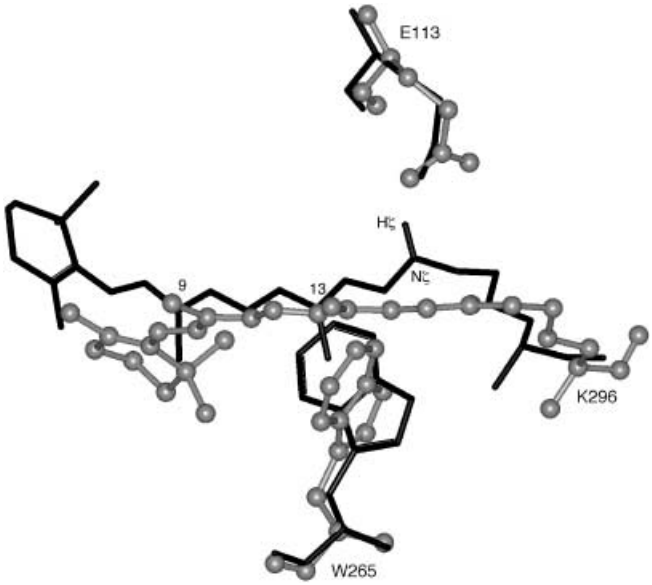

Figure 4. Superimposed conformations of the chromophore in the lumirhodopsin (gray ball and stick) and metarhodopsin I (black stick) models (view from the extracellular site). Only three residues (E113, W265, and K296) and the PSB proton (Hζ) are shown for clarity. Downward (lumirhodpsin) and upward (metarhodopsin I) twists of chromophore indicate left- and right-hand twists, respectively.

and is consistent with the CD signal band of metarhodopsin I.[11, 38] Thus, the metarhodopsin I model built by the swing of the C-terminal portion of TM3 would yield a chromophore structure that would account for the observed spectral data.

The swing of TM4 appears to be necessitated by steric interactions with the large Trp126 residue on TM3 and the cyclohexenyl group and suggests that the kinked portion caused by Pro171 works like a flexible joint, to leave the C-terminal

portion and the following extracellular loop 2 unchanged (Figure 5). The flexible structure of the kinked site would coincide with deformation of this site by the bulky, modified cyclohexenyl group.[7, 13]

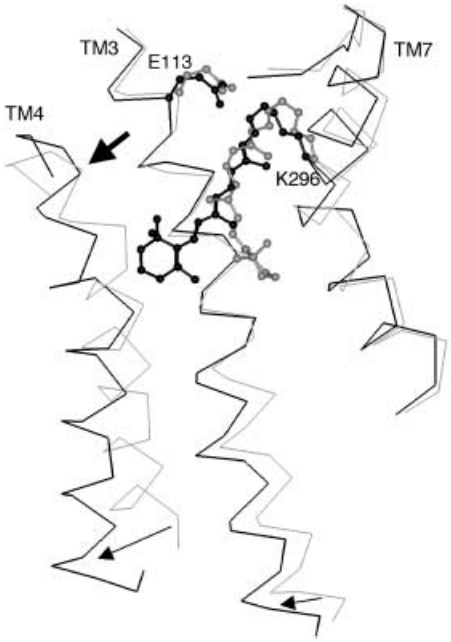

Figure 5. *Motion of TM3 and TM4 in the metarhodopsin I model. Cα traces for TM3, TM4, and TM7, the chromophore, and two residues of metarhodopsin I are shown in black. The corresponding structures of the rhodopsin crystal are shown in gray. Thin arrows indicate the direction of motion of TM3 and TM4. The thick arrow indicates the position of the flexible joint (P171) for the swing of the N-terminal end of TM4.*

The outward motion of TM3 yielded a space for about ten water molecules at the intracellular site. The EPR measurements on the rhodopsin mutants, in which a spin-labeled Cys residue is introduced at the intracellular site, did not detect a significant change of the mobility of the spin-labeled moiety in the metarhodopsin I state arrested in digitonin.[39] The rather small outward motion would not largely affect the mobility of the spin-labeled moiety that might not be introduced at specific sites for detecting the structural changes of metarhodopsin I. The uptake of water molecules into the space might contribute to the stability of metarhodopsin I and partly to the negative entropy change in the formation of metarhodopsin I.[34, 40]

A similar swing of TM3 but not of TM6 provided a space for the C11 – C13 fused 5-membered-ring analogue of 9-*cis*-retinal in the model of the rhodopsin analogue and accounted for an unusual photoisomerization of the analogue chromophore.[14] The ring introduced into the chromophore required an expansion of the chromophore binding cleft of opsin to avoid unfavorable steric interactions. Interaction between the 9-methyl group and Gly121 on TM3 was proposed as a trigger of rhodopsin activation.[41] In light of the crystal structure of rhodopsin,[25–27] Gly121 is not close to the 9-methyl group, but it is close to the Trp265 residue. The substitution of Ala or Ile for Gly121 yields steric interactions with Trp265 and the 5-methyl group of the chromophore. These interactions would be similar to those encountered in the ring-fused analogue-bound rhodopsin.[14] The 9-ethyl and 9-propyl retinal analogues also cause severe steric interactions with Thr118 on TM3. Thus, the 9-methyl group and mutants at Gly121 would independently trigger the expansion of the chromophore binding cleft and would lead to receptor activation.

The present assumption that the C-terminal portion of TM3 swings outward would contrast with the results shown by a 10 ns molecular dynamics study of primary photoinduced events, which suggests high mobility of TM6, but not of TM3 and TM4.[42] TM6 is most loosely associated with other transmembrane helices in rhodopsin,[43] although the temperature factors for the residues on TM6 are not particularly high among the residues on transmembrane helices. The molecular dynamics simulation would not reach an event which involves motions of TM3 and TM4 since bathorhodopsin decays to lumirhodopsin over 150 ns. In addition, a few detergent molecules specifically bind near TM6 in the crystal structure (PDB ID codes: 1HZX, 1L9H).[26, 27] Under physiological conditions, lipid molecules would associate with transmembrane helices and would play a critical role in the mobility of TM6 at the lipid – TM6 interface.

Although our assumption regarding the motion of TM3 appears to be consistent with the spectral data for the photointermediates, further experimental evidence would be required to verify the models.

Model building of the photointermediates in the late photocascade

The crystal structure of rhodopsin does not provide direct information about the activated structure, metarhodopsin II, although it affords considerable structural information, particularly about the highly conserved residues. Here, we made the following assumptions for modeling of metarhodopsin I_{380} and metarhodopsin II. 1) The structure of the three-helix bundle of TM1, TM2, and TM7 remains unchanged during the photochemical process. The conserved residues, Asn55, Asp83, Asn302, and Pro303 in the interior region of the three-helix bundle form a hydrogen-bond network that contributes to maintenance of the three-helix bundle. Try306 on TM7 forms a hydrophobic core with residues at the intracellular ends of the three-helix bundle and the intracellular helix, H8. The hydrogen bond between Tyr306 and Asn73 on TM2 also contributes to the maintenance of the three-helix bundle at the intracellular site. 2) The highly conserved Cys110 residue acts as a pivot in the outward swing of TM3. The Cys residue is locked at the N-terminal end of TM3 by forming a disulfide bond with Cys187 on the second extracellular loop. 3) The kinked portion at Ala168 through to Leu172 plays a flexible joint-like role in the swing of TM4. The modeling study of lumirhodopsin and metarhodopsin I described above suggested that the kinked portion at Pro171 becomes a flexible joint for the swing of the N-terminal end of TM4. 4) The hydrogen bonds formed by Arg135 with Glu134 and Glu247 at the intracellular site participate in the control of movement of the C-terminal end of TM3 relative to TM6. Arg135 of the highly conserved Glu134 –

Arg135 – Tyr136 (ERY) triplet forms hydrogen bonds with Glu134 and Glu247 on TM6 in the crystal structure and contributes to a tight binding of TM3 with TM6 at the intracellular site.[44]

The chromophore conformation in the lumirhodopsin model described above had contacts between the *gem*-dimethyl group at C1 and Trp265 and between the 9-methyl group and Tyr191. We postulated that a further swing of TM3 would lead to the subsequent photointermediate, metarhodopsin I_{380}, at physiological temperatures.

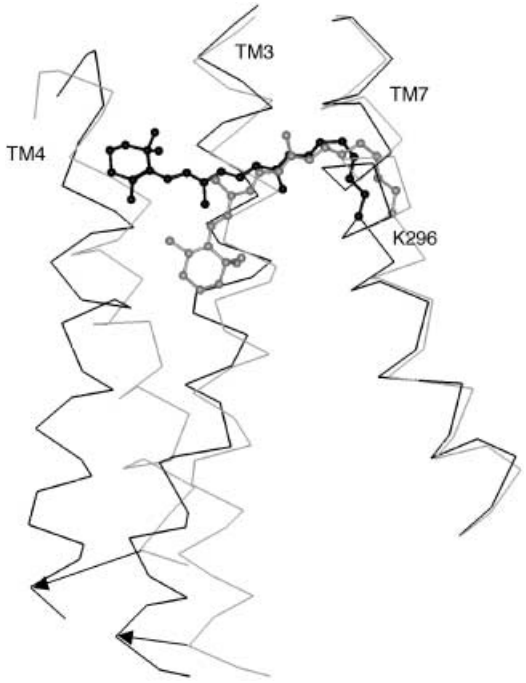

Figure 6. *Motion of TM3 and TM4 in the metarhodopsin I_{380} model (lateral view; the extracellular site is at the top). Cα traces for TM3, TM4, and TM7, the chromophore, and K296 of metarhodopsin I_{380} are shown in black. The corresponding structures of the lumirhodopsin model are shown in gray. The directions of the motion of TM3 and TM4 are indicated by arrows.*

A putative structural model of metarhodopsin I_{380}

At physiological temperatures, lumirhodopsin rapidly equilibrates with metarhodopsin I_{380},[22] which has a neutralized form of the Schiff base as judged from its absorption maximum (380 nm). Neutralization of the Schiff base would render TM3 highly mobile, since ionic interaction between the PSB and the counterion confines the motion of TM3 within a limited range. Although the range of the swing of TM3 is unknown, we assumed the following to define the swing of TM3. 1) Arg135 holds a hydrogen bond with Glu247 on TM6 at a maximum distance between TM3 and TM6, since the hydrogen bond plays an important role in maintenance of the inactive structure as found in the crystal structure.[44] 2) The carboxylic acid of Glu113 is located more than the hydrogen-bond-forming distance (>3.3 Å) from the Schiff base, while it maintains the hydrogen bond with the main-chain amide of Cys187.

Examining the outward swing of TM3 pivoting on Cys110, we found that an outward motion of the C-terminal portion by 6 Å satisfies the conditions that Arg135 can form a hydrogen bond with Glu247 while the carboxyl oxygen atom of Glu113 is located 3.4 Å from the Schiff base nitrogen. The outward motion of TM3 provoked a collision with TM4, while the interhelical contact between TM3 and TM5 was lost at the intracellular site (from 6.2 Å to 12.2 Å between Tyr136 and Cys222 in rhodopsin and in the metarhodopsin I_{380} model, respectively). As suggested in the metarhodopsin I-like structure model with the retinal analogue modified for the photoaffinity-labeling experiments, the kinked portion caused by the conserved Pro171 residue, as well as the adjacent Pro170, would be sufficiently flexible to bend the N-terminal portion of TM4.[13] The swing, pivoting at Leu172 and Ala168, gave an appropriate disposition of the N-terminal end of TM4 to avoid collision with TM3 and plug the sparse interface between TM3 and TM5. Thus, the structural change initiated by the swing of TM3 at Cys110 was compensated for by bending at the kink portion caused by Pro170 and Pro171 on TM4. The final structural model for metarhodopsin I_{380} showed movements of about 9.5 Å and 20 Å for the intracellular ends of TM3 and TM4, respectively (Figure 6). The large motion of 20 Å may not be exceptional, since transmembrane helices probably move about 15 Å during the activation of erythropoietin receptor upon binding erythropoietin.[45] On the other hand, the swings of TM3 and TM4 did not largely affect the conformation of the extracellular loops, since the intracellular portions of TM3 and TM4 tilted, pivoting at the extracellular ends of the helices. The motion of TM4 towards TM5 resulted in a helix arrangement unlike that of rhodopsin at the intracellular site. In other words, the N-terminal portion of TM4 rearranged to plug the interface between TM3 and TM5 in the photointermediate model. The tilts of TM3 and TM4 against TM2 in the metarhodopsin I_{380} model were 170° and 25°, respectively, whereas those in rhodopsin were 160° and −25°. This switch of the arrangement should cause a large conformational change of the second intracellular loop connecting TM3 and TM4. The outward swing of TM3 brought about a considerably large pore enclosed by the seven transmembrane helices at the intracellular site. This pore had a volume roughly equivalent to 35 water molecules (not shown). Glu134 of the highly conserved ERY triplet on TM3 was transferred to the hydrophobic phase at the interface between two helices (TM2 and TM3) and a lipid phase (Figure 7). At this interface, Glu134 is surrounded by hydrophobic residues on both helices, such as Pro71 on TM2 and Val130, Leu131, Ile133, Val137, and Val138 on TM3, as well as lipids. This environment would stabilize the protonated Glu134 residue and Arg135 would thus easily switch the hydrogen bond from Glu134 to Glu247. The remaining Tyr136 residue of the triplet forms a hydrophobic core with hydrophobic residues, such as Ile133 and Cys140 on TM3, Gly149, Ala153, and Val157 on TM4, and Val218 and Cys222 on TM5 (Figure 7). We thus speculate that Tyr136 contributes to stabilizing the new helical arrangement of TM3 and TM4 at the intracellular ends. Trp126 on TM3 was displaced from the retinal binding cleft to the lipid phase and faced Trp161 across the interface between TM3 and TM4 (Figure 7). The dislocation of Trp126 caused a new hydrogen bond between Glu122 on TM3 and His211 on TM5. These two residues form a

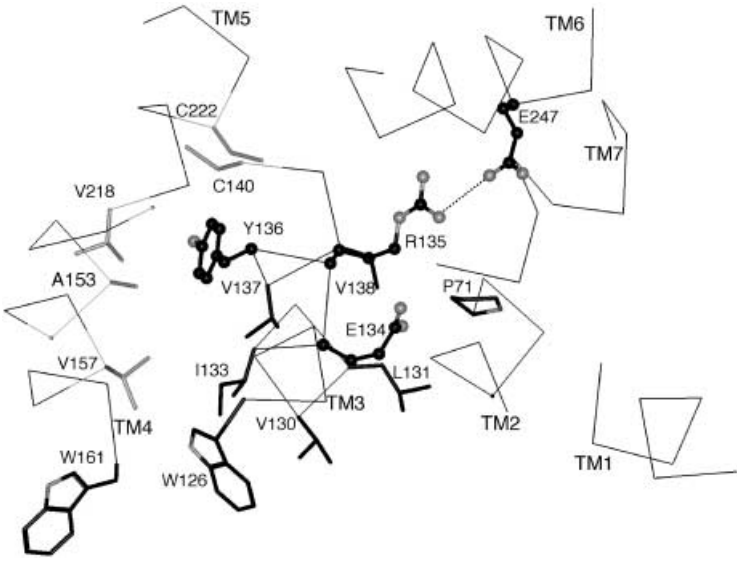

Figure 7. Residues neighboring the ERY triplet and two tryptophan residues (W126 and W161) on TM3 and TM4 (view from the intracellular site). The ERY triplet and E247 are depicted as ball-and-stick models. Residues surrounding E134 are black sticks and those surrounding Y136 are gray sticks. The hydrogen bond is indicated by a dotted line.

hydrogen-bond network mediated by Trp126 in the rhodopsin crystal. The aromatic – aromatic interaction and the hydrogen bond would also contribute to the stabilization of the helical arrangement of TM3 through TM5.

The chromophore showed an entirely flipped conformation of the β-ionone moiety at the C11–C12 double bond (Figure 8). The polyene plane with a flat conformation was almost as parallel to a membrane plane as that of rhodopsin and the metarhodopsin I model. Thus, the space generated by the motion of TM3 and TM4 enabled the conformation of the chromophore to change. The cyclohexenyl moiety fitted into the pocket formed with Thr118 on TM3, Cys67 and Pro170 on TM4, and Met207 on TM5. The 9-methyl group pointed towards Trp265 at a distance of 3.9 Å and the 13-methyl group pointed towards Ala295 on TM7 at a distance of 4.2 Å. The lone pair of Schiff base nitrogen atom was oriented towards the carboxylic acid oxygen atom of Glu113 at a distance of 3.3 Å (Figure 8).

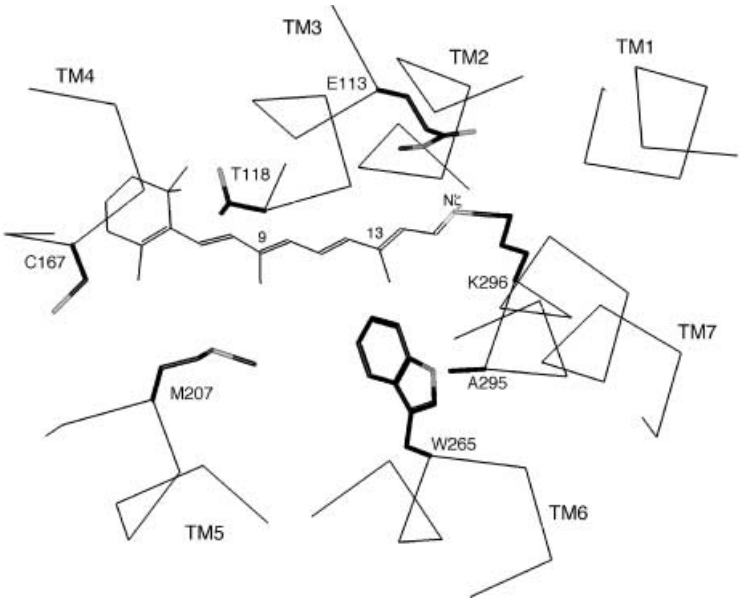

Figure 8. Conformation of the chromophore in the metarhodopsin I_{380} model (view from the extracellular site). Selected residues neighboring the chromophore are shown by stick models. Hydrogen atoms except for the carboxylic acid of Glu113 are neglected for clarity.

Since metarhodopsin I_{380} is a short-lived photointermediate, whether it binds transducin or facilitates the guanosine diphosphate – guanosine triphosphate (GDP – GTP) exchange remains unclear. However, the protonated form of Glu134 would be stabilized in the apolar environments described above. Hence, a stable metarhodopsin I_{380}-like structure might bind transducin and facilitate the GDP – GTP exchange. The substitution of Gln for Glu113 should reduce the electronic interaction between TM3 and TM7 and would render TM3 mobile. Although the Glu113Gln mutant has high constitutive activity, it has only half the activity of a fully activated metarhodopsin II-like protein.[46, 47] Since the mutant is convertible to a fully active or inactive structure by adding either all-*trans*-retinal or 11-*cis*-retinal, respectively,[46–48] the protein structure of the mutant would not be analogous to that of metarhodopsin II or rhodopsin, but rather to the metarhodopsin I_{380} model. Thus, metarhodopsin I_{380} might be able to bind transducin.

Structural model of metarhodopsin II

Large structural changes are accompanied by rigid-body movements of the transmembrane helices during the formation of metarhodopsin II.[15, 39, 49–54] Rotation of TM6 has been attempted at an early stage of the photoisomerization (that is, ≈10 ns) by means of steered molecular dynamics.[43] This showed that TM6 has the potential to rotate about a helix axis. However, TM6 appears to be rotated later, since metarhodopsin I does not show a large structural change according to the EPR experiments.[39] Therefore, we postulated that the major rigid-body rotation occurs during the metarhodopsin I_{380} to metarhodopsin II transition.

Reduction of the tertiary interaction between TM3 and TM6 at the intracellular site during the formation of metarhodopsin II[49] indicates that TM3 and TM6 are not as tightly bound in metarhodopsin II as they are in rhodopsin. The protein in the metarhodopsin I to metarhodopsin II transition increases in volume by roughly the same amount as in the formation of lumirhodopsin at physiological temperatures.[5, 6] As described above, the metarhodopsin I_{380} model had a wide-open pore enclosed by seven transmembrane segments at the intracellular site. The volume (about 1020 Å^3) of this pore is about 40% of that of TM6 (Gln246 – Ile263). Hence, the wide-open pore of metarhodopsin I_{380} at the intracellular site would become

compact during the metarhodopsin I_{380} to metarhodopsin II transition.

The exposure of a fairly large region of the hydrophobic interior of opsin to the aqueous phase due to the outward swing of the C-terminal portion of TM3 led us to assume that TM6 translates towards TM3 to restore hydrophobic interactions at the protein interior. However, TM5 interfered with the inward translation of TM6 by sterically interacting with the extracellular portion of TM6 kinked by the highly conserved Pro267 residue. This unfavorable steric interaction could be avoided by the clockwise rotation of TM6 about its helical axis (as viewed from the intracellular site). TM6 is most loosely associated with other transmembrane helices in rhodopsin.[43, 44] The outward swing of the intracellular portion of TM3 gave more space for TM6 to rotate. Thus, the steric interactions between TM5 and TM6 provide a structural basis for the rigid-body rotation of TM6 that was observed in site-directed EPR experiments.[15] Since the substitution of Pro267 with amino acid residues other than Gly significantly reduced the activity,[35] the structure of TM6 kinked at Pro267 would play an indispensable part in the metarhodopsin II formation.

A clockwise rotation (about 100° from the intracellular site) of TM6 about the axis of the N-terminal portion (Lys245 – Cys264) provided a suitable arrangement to avoid steric interactions with the extracellular portions of TM5 and TM7. The C-terminal portion of TM6 (Tyr268 – Tyr274) became parallel (about 170°) to the N-terminal portion of TM7 (Met288 – Ser298) kinked by Pro303. Thus, control of the rigid-body rotation of TM6 might be one of the roles of the highly conserved Pro303 residue. A concomitant inward translation of TM6 (by about 5 Å) provided a metarhodopsin II model (Figure 9), in which Ala246 on TM6 faces towards Val139 on TM3 with a distance of 8 Å between their β carbons (Figure 10). The distance is longer than that between Val139 and Glu247 in the rhodopsin crystal structure (5.6 Å).

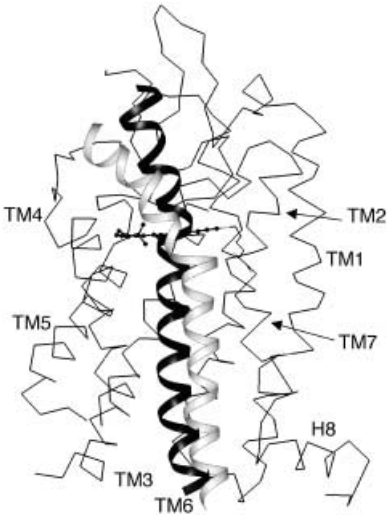

Figure 9. *Motion of TM6 (lateral view; the extracellular site is at the top). Gray and black ribbon models are TM6 in the metarhodopsin I_{380} and metarhodopsin II models, respectively. For clarity, only the retinylidene chromophore and K296 are shown.*

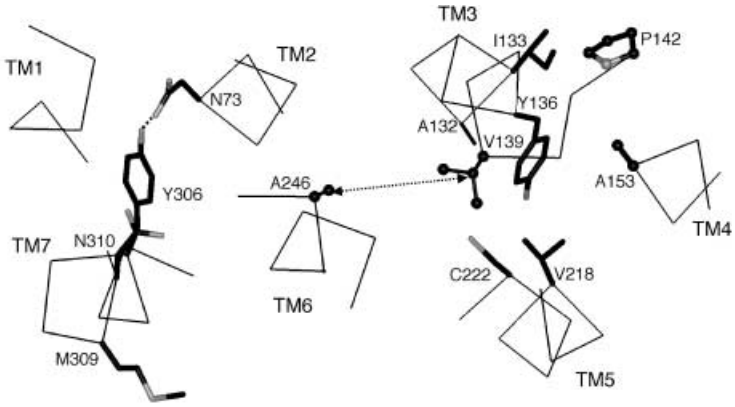

Figure 10. *Selected residues at the intracellular site in the metarhodopsin II model (view from the intracellular site). V139, A153, and A246 are shown by ball-and-stick models. Heteroatoms (N, O, and S) are colored gray. The dotted arrow indicates the distance between Cβ atoms and the hydrogen bond between N73 and Y306 is indicated by a dotted line.*

Ala153 on TM4 increased tertiary interaction with residues on TM3 and TM5, such as Ala132, Ile133, and Tyr136 on TM3 and Val218 and Cys222 on TM5, by moving the N-terminal portion of TM4 towards the helical interface between TM3 and TM5 (Figure 10). This is consistent with the motion predicted from the EPR measurement on a spin-labeled mutant substituted at Ala153 on TM4.[49] At another site, the residues Tyr306, Met309, and Asn310 on TM7, located at the intracellular interface between TM6 and TM7, were exposed to the aqueous phase (Figures 10 and 12). Observation of the light-induced exposure of the C-terminus residues, in particular, Tyr306, Met309, and Asn310 on TM7,[55] coincided with exposure of these residues to the aqueous phase in the metarhodopsin II model. Since Tyr306 forms a hydrogen bond with Asn73 on TM2 in the crystal structure, the hydrogen bond should be weakened by Tyr306 being exposed to the aqueous phase. The exposure of those residues to the aqueous phase may render the residues mobile. The increase in mobility of those residues is consistent with the alteration of the distances in double spin-labeled mutants at those specific residues.[52, 53]

The rigid-body rotation of TM6 would provoke a considerable structural change at the third extracellular loop. A wide space due to reorientation of the C-terminal portion of TM6 from the N-terminal end of TM5 to that of TM7 would allow the second extracellular loop, which is tightly plugged in the chromophore binding site in rhodopsin, to gain mobility. This is consistent with the observations that Cys185 on the second extracellular loop is labeled only upon illumination[56] and that hydroxylamine, which does not react with the PSB of rhodopsin, readily reacts with the Schiff base upon illumination.[48] The rigid-body rotation of TM6 considerably changes the chromophore binding pocket and the conformation of the third intracellular loop. Diffusible ligands of the rhodopsin family of GPCRs bind at a similar site to that where the retinylidene chromophore binds[57] and the agonists and antagonists recognize different amino acid residues on TM6. For example, acetylcholine binds Tyr403 on TM6 of the muscarinic

acetylcholine receptor (M_2R) but not Asn404, whereas the antagonist, *N*-methyl scopolamine, binds Asn404 but not Tyr403.[58, 59] Thus, the structural change in the photocascade of rhodopsin would correlate with that in the activation of GPCRs of the rhodopsin family.

The present picture for the motion of the transmembrane region appears to be consistent with the experimentally observed data. Together with a view in agreement with our picture, Altenbach et al proposed a different picture for the motion of the transmembrane helices, in which they postulate the outward motion of TM2, TM6, and TM7.[52] However, with respect to the outward motion of TM6, the outward motion of TM3 affords the same consequence of the reduction of a tertiary interaction between TM3 and TM6. The metarhodopsin II model indicated that the outward motion of the intracellular portion of TM3 is larger than the inward motion of TM6, thereby leading to a decrease in tertiary interaction between TM3 and TM6. As described above, the outward motion of TM3 to form the structural models of lumirhodopsin and metarhodopsin I afforded a conformational change of the chromophore consistent with that observed from the laser-Raman spectra.[56] An unusual photoisomerization of a C11 – C13 ring-fused retinal bound to opsin was also suitably adapted to the outward motion of TM3, but not to the outward motion of TM6.[14] Crystallographic analyses of the photointermediates in the bacteriorhodopsin photocycle have shown that TM6 has outward motion in the all-*trans* to 13-*cis* isomerization.[60, 61] This indicates that the 13-*cis* to all-*trans* isomerization for restoring the initial chromophore structure causes the inward movement of TM6 in the photocycle. In the rhodopsin photocascade, the 11-*cis*-retinylidene chromophore isomerizes to the all-*trans* chromophore. Thus, irrespective of the position of the *cis* double bond in the retinal chromophore, inward motion of TM6 in the rhodopsin photocascade and the bacteriorhodopsin photocycle would be common in the *cis* to *trans* isomerization of the retinylidene moiety. With respect to the motions of TM2 and TM7, exposure of the interhelical interface between TM2, TM6, and TM7 to the aqueous phase render the specific residues at 73 (TM2), and 306 and 310 (TM7) mobile and the spin-labeled residues should gain flexibility at these positions with altered distances between them. Thus, the present model suggests that the formation of metarhodopsin II does not require the outward motion of the intracellular portions of TM2 and TM7. This appears to agree with the finding that the disulfide cross-links in the intracellular site of rhodopsin do not prevent transducin activation.[62]

The conformation of the chromophore was similar to that of metarhodopsin I_{380}. The 9- and 13-methyl groups point towards TM6 and TM7, respectively (Figure 11). Although the chromophore shows an almost flat conformation, it exhibited slight positive twists (178° and 176°) at the C12—C13 and C14—C15 bonds, while the C8—C9 and C10—C11 bonds held no twists. These positive twists suggest that the right-twisted conformation of the chromophore is consistent with the positive CD band observed at 380 nm for the metarhodopsin II of bovine rhodopsin.[11]

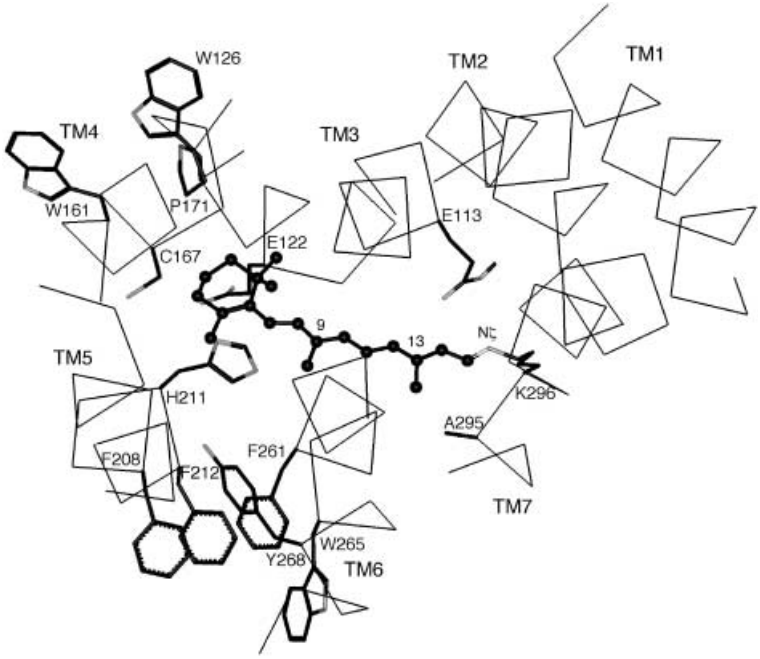

Figure 11. *Location of three tryptophan residues (W126, W161, and W265) and four aromatic residues (F208, F212, F216, and Y268) at the protein – lipid interface and residues at the pocket for the cyclohexenyl group (view from the extracellular site). The chromophore is shown by a ball-and-stick model. Only the hydrogen atom on the carboxylic acid of E113 is shown for clarity.*

The displacement of Trp126 on TM3 from the chromophore binding cleft, where Trp126 forms a hydrogen-bond network with Glu122 and His211 in rhodopsin, to the lipid phase accounts for the weaker hydrogen bonding of the indole N—H group in metarhodopsin II.[63] Glu122 was located within hydrogen-bond-forming distance of His211. This hydrogen bond would contribute to a higher stability of rhodopsin than of red and green cone pigments that have nonacidic residues at an analogous position to Glu122.[64] Trp265 is also transferred to the lipid phase from an apolar cyclohexenyl moiety binding site in rhodopsin (Figure 11). The indole moiety would be proximal to the polar head of lipids, since a linear dichroism study of UV-difference bands indicates a reorientation of an indole side chain from an apolar to a polar environment in the formation of metarhodopsin II.[63] The Trp residue at the lipid phase would contribute to the stabilization of metarhodopsin II, since Trp is often found at the lipid phase in the crystal structures of membrane proteins.[65] Moreover, Phe208, Phe212, Phe261, and Tyr268 form an aromatic cluster at the helical interface between TM5 and TM6 (Figure 11). This aromatic interaction would contribute to the stability of metarhodopsin II.

The Glu134 residue of the ERY triplet was surrounded by hydrophobic residues such as Pro71, Tyr74, Val130, Leu131, Val137, and Val138 at the interface between TM2 and TM3 and was exposed to the lipid phase as described in the metarhodopsin I_{380} model (Figure 12). A neutralized form of Glu134 would be stabilized at this hydrophobic interface and would

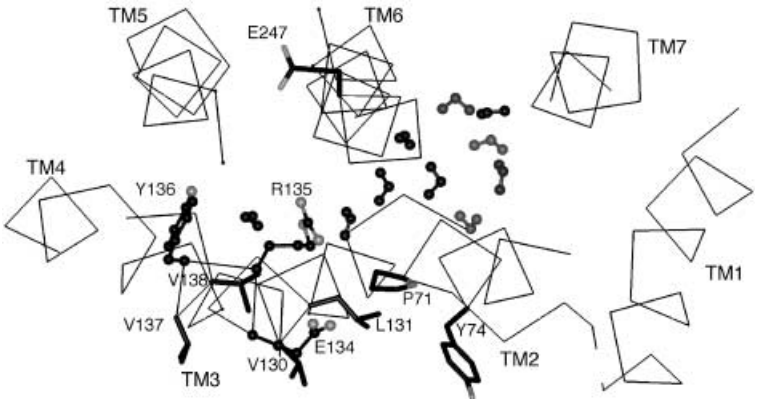

Figure 12. *Residues surrounding E134 of the ERY triplet at the protein – lipid interface and water molecules at the intracellular pore (view from the intracellular site). The ERY triplet and water molecules are shown by ball-and-stick models.*

enable Arg135 to change its conformation and become exposed to the aqueous pore enclosed by the transmembrane helices for interacting with transducin or other residues on the intracellular loops. Thus, the outward motion of the C-terminal portion of TM3 provides a structural basis for the protonation of Glu134 at the intracellular site of metarhodopsin II.[20] The protonation of ionized Glu134 in the metarhodopsin IIa state affords the fully activated metarhodopsin IIb form shown in Figure 12. On the other hand, Glu247 on TM6, which forms a hydrogen bond with Arg135 in the crystal structure of rhodopsin, may maintain an ionized form and would contribute to the formation of photointermediates prior to the formation of metarhodopsin II. Tyr136 of the ERY triplet would participate in the stabilization of metarhodopsin II by forming a hydrophobic cluster as described in the metarhodopsin I_{380} model (Figure 7). Although data about a Tyr136 mutant is unavailable, an indispensable role of the aromatic moiety of the D(E)RY triplet in the G-protein activation in the bradykinin receptor would be in agreement with the putative role of Tyr136 in rhodopsin.[66]

Structural model of metarhodopsin Ib with correlation to wild-type opsin

The large structural change between the metarhodopsin I and metarhodopsin II models described above is in agreement with that detected by EPR measurements. During the metarhodopsin I to metarhodopsin II transition, the intermediate, metarhodopsin Ib, has been characterized by time-resolved UV spectroscopy.[23, 24] The protein moiety, opsin, binds but does not activate transducin, even though the chromophore maintains the protonated form of the Schiff base with a UV absorption maximum at 470 nm.[24]

We assumed the following to build a model of the metarhodopsin Ib structure. 1) The tilt of TM3 is intermediate between those of metarhodopsin I and metarhodopsin II since it is an intermediate in the metarhodopsin I to metarhodopsin II transition. 2) The PSB is located within hydrogen-bond-forming distance (≈2.8 Å) of its counterion, Glu113. 3) Glu134 on TM3 is ionized and maintains a salt bridge with a protonated form of Arg135 as found in rhodopsin, since metarhodopsin Ib binds only the inactive form of transducin. 4) Glu247 on TM6 maintains a hydrogen bond with Arg135, thereby leading to a maximum distance between TM3 and TM6 in the intermediate, since the hydrogen bond would confine the distance between TM3 and TM6.

An extended side-chain conformation of Glu247 enabled the intracellular end of TM3 to swing outward about 2 Å from the metarhodopsin I structure. Since TM4 swung at the kinked portion as a flexible joint in the modeling of metarhodopsin I, the N-terminal end of TM4 towards TM5 was swung manually to remove roughly the steric interactions with TM3 by bending the kinked portion at Ala168 and then the structure was minimized. Thus, the intracellular portion of TM4 moved about 11 Å from that of the metarhodopsin I model. The fairly large conformational changes of TM3 and TM4 would cause a considerable conformational change of the second intracellular loop, which will then be recognized by transducin. The fairly large displacement of the intracellular end of TM3 from that of rhodopsin (about 5 Å) generated a large pore, which is equivalent to the volume of at least 15 water molecules (Figure 13). However, Glu134 would remain ionized and would not allow Arg135 to form a conformation that would activate transducin, since Glu134 was not transferred to the lipid phase. The outward motion of TM3 provided more space for the conformational change of the chromophore to reduce the steric interaction between Trp265 and the chromophore. Thus, Trp265 restored the original conformation in the lumirhodopsin model. This suggests that steric interaction between Trp265 and the 9-methyl group contributes to the structural change of metarhodopsin I.

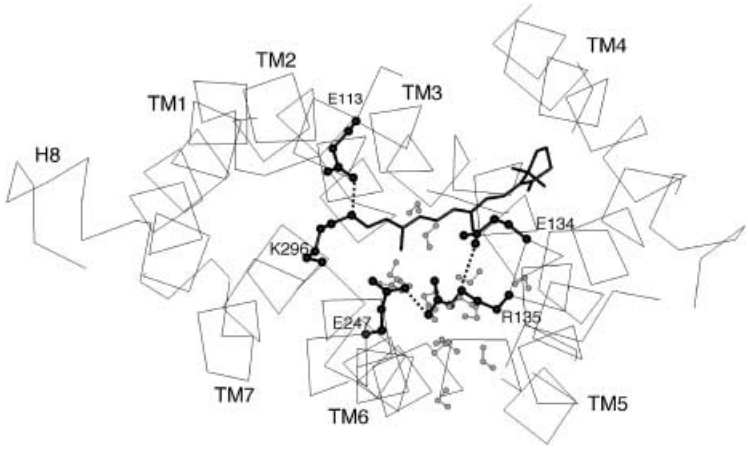

Figure 13. *The hydrogen-bond network and water molecules at the intracellular pore formed in the metarhodopsin Ib model (view from the intracellular site). TM regions are depicted by Cα traces. Specific residues are shown as black ball-and-stick models and water molecules are smaller ball-and-stick models. Dotted lines indicate hydrogen bonds. Hydrogen atoms except for water molecules are omitted for clarity.*

The conformation of the polyene moiety of the chromophore was more right-twisted and maintained a hydrogen bond between the PSB and Glu113. The 9-methyl group is surrounded by Ile189 on the second extracellular loop, Met207 on TM5, and Trp265 and Tyr268 on TM6 (Figure 14). Eliminating the contacts

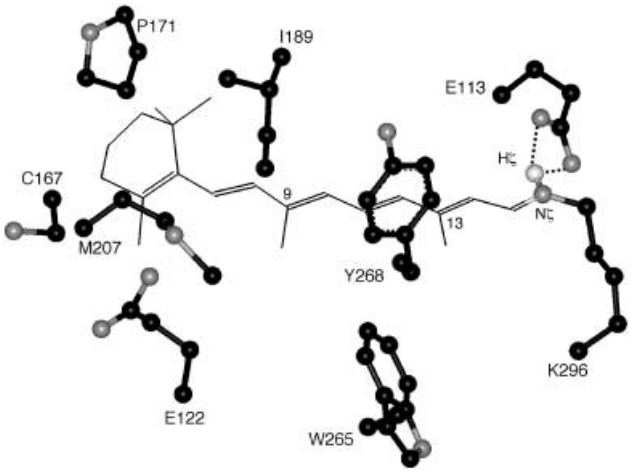

Figure 14. *Conformation of the chromophore and surrounding residues in the metarhodopsin Ib model (view from the extracellular site). Heteroatoms (N, O, and S) are shown in gray. Hydrogen atoms except for the PSB proton are neglected for clarity. Dotted lines indicate hydrogen bonds.*

with these residues would reduce a further structural change and stabilize the metarhodopsin Ib-like structure of the photoproduct. This agrees with the observation that the photoactivation of 9-demethyl retinal-bound rhodopsin fails to convert the protein into the metarhodopsin II state under near physiological conditions.[36] The final photoproduct activates transducin to only 8% of the fully activated rhodopsin, metarhodopsin II. A similar weak activation of transducin by wild-type opsin indicates that wild-type opsin also binds transducin to elicit its activity.[67] The complete loss of the activity by binding 11-*cis*-retinal implies that wild-type opsin has a structure distinct from that of rhodopsin. Since wild-type opsin would form a salt bridge between Glu113 and Lys296, it presumably has a structure analogous to that of metarhodopsin Ib.

Conclusion

The conformations of the retinylidene chromophore generated in the structural models of lumirhodopsin and metarhodopsin I were in good agreement with the structural data obtained from FTIR, laser Raman, and CD spectra and accorded with the assumptions on the motion of TM3 and TM4. During interactions between the chromphore and the protein moiety, the 9-methyl group and Trp265 in the metarhodopsin I model would be noteworthy since both groups appear to play important roles in the structural change. An extension of the motion of TM3 and TM4 led to structural models of the photointermediates, such as metarhodopsin Ib, metarhodopsin I_{380}, and metarhodopsin II at a later stage. The model of metarhodopsin II built from that of lumirhodopsin through metarhodopsin I_{380} satisfied experimental results such as EPR spectra of spin-labeled rhodopsin mutants. The photointermediate models provided a plausible structural basis for the rigid-body rotation of TM6 and the protonation of Glu134 in metarhodopsin II.

Hence, we summarize putative roles of the highly conserved residues for the structural change of the rhodopsin photocascade. The conformational changes observed are possible without disrupting the conformation of the disulfide bond between Cys110 and Cys187 and the conformation of the extracellular portion of TM4 where the kink by Pro171 would serve as a flexible joint at the C-terminal end of TM4 in the swing of TM4. The electrostatic change at the extracellular site (that is, the neutralization of the PSB) caused by the photochemical isomerization of the 11-*cis*-retinylidene chromophore would be thus conveyed to the intracellular surface through the displacement of Glu134 and Arg135 on TM3 from polar to apolar environments. Tyr136 may contribute to stabilizing the metarhodopsin II state through the formation of a hydrophobic core at the intracellular ends of TM3 and TM4. Pro267 would have an important role in the rigid-body rotation of TM6. Trp265 on TM6 would participate in stabilization of the metarhodopsin II state. The formation of metarhodopsin II would not require motion of the three-helix bundle of TM1, TM2, and TM7 that forms the hydrogen-bond network between Asn55, Asp83, and Asn302 and between Asn73 and Tyr306.

Experimental Section

The bathorhodopsin model[13] was used as the starting structure for the model building of lumirhodopsin. The metarhodopsin I and metarhodopsin I_{380} models were built starting from the lumirhodopsin model, while the metarhodopsin Ib model was derived from the metarhodopsin I model. The C-terminal end of TM3 was gradually swung towards TM4, pivoting on Cys110. The steric interactions caused by the motion of TM3 were then removed by structure minimization on the protein structure. Interhelical $C\alpha$–$C\alpha$ distances between TM2 and TM3 were maintained above 4.5 Å. The minimum interhelical $C\alpha$–$C\alpha$ distance was estimated from interhelical distances of crystal structures of membrane proteins (Y. Oyama and M. Ishiguro, unpublished results). The intracellular pore generated by the motion of TM3 and TM4 was filled with water molecules by using the Assembly module installed in the Insight II package (Molecular Simulations Inc., San Diego, CA).

Molecular dynamics calculations for each structure within the chromophore binding site (residues within 10 Å from the chromophore) were performed at 300 K by using a cell multipole method, a distance-dependent dielectric constant, and a time step of 1 fs for 100 ps by sampling the conformation every 1 ps by using the CVFF parameters in the Discover 3 program (version 98, Molecular Simulations Inc., San Diego, CA). The entire structure of the selected model was minimized until the final root-mean square deviation became less than 0.1 kcal mol^{-1} $Å^{-1}$.[68]

Modeling of the photointermediates, lumirhodopsin and metarhodopsin I: The conformations of TM3 for the model of lumirhodopsin were generated by swinging the C-terminal end of TM3 every 0.2 Å from the structural model of bathorhodopsin.[13] A TM4 region (148–173) was minimized for every protein structure to remove bumps with TM3. TM3 was swung by 1.4 Å and then the pore formed at the intracellular site was filled with water molecules. The final

structural model of lumirhodopsin was energy minimized and the conformation of the chromophore was optimized by the molecular dynamics/minimization procedure.

The C-terminal end of TM3 was further swung every 0.2 Å by 2.0 Å from the structural model of lumirhodopsin. The following structure minimization of the TM4 region afforded a structural model of metarhodopsin I. After filling the pore with water molecules, the initial structural model of metarhodopsin I was energy minimized and the conformation of the chromophore was optimized by the molecular dynamics/minimization procedure.

Modeling of the photointermediates, metarhodopsin I_{380} and metarhodopsin II: The conformation of TM3 for the model of metarhodopsin I_{380} was generated by swinging the C-terminal end of TM3 by 6.6 Å from the lumirhodopsin model. The N-terminal end of TM4 was then swung to 20 Å to plug the space between TM3 and TM5 generated by the movement of TM3, pivoting on Ala168 to reach an interhelical contact with TM5. After filling the pore formed at the intracellular site with water molecules, the initial structure was energy minimized. The conformation of the chromophore was then optimized by the molecular dynamics/minimization procedure.

TM6 of the metarhodopsin I_{380} model was rotated counterclockwise (as viewed from the extracellular site) about the axis of the N-terminal helix consisting of Lys245 – Cys264 and collisions with the neighboring N-terminal portion of TM7 were examined. TM6 was then translated towards TM3 until a van der Waals contact was generated with TM3 and TM5, while maintaining a $C\alpha$–$C\alpha$ distance to TM7 of more than 4.5 Å. The initial structure was filled with water molecules at the pore of the intracellular site, the structure was minimized, and then the conformation of the chromophore was optimized as described above.

Modeling of a metarhodopsin Ib model: The C-terminal end of TM3 was swung to within hydrogen-bond-forming distance between Arg135 on TM3 and Glu247 on TM6, with the salt bridge between Gul134 and Arg135 maintained as observed in the crystal structure. The N-terminal end of TM4 was swung towards TM5, pivoting on Ala168 to remove the collision with TM3. The intracellular pore was filled with water molecules and then the protein moiety was energy minimized. The conformation of the chromophore was optimized by the molecular dynamics/minimization procedure.

Acknowledgements

This study was supported by grants from the Special Coordination Fund for the Promotion of Science and Technology from the Ministry of Education, Culture, Sports, Science, and Technology and from CREST of Japan Science and Technology Agency.

Keywords: G-protein-coupled receptors · lumirhodopsin · metarhodopsin · rhodopsin · membrane proteins

[1] H. G. Khorana, *J. Biol. Chem*. **1992**, *267*, 1 – 4.
[2] Rhodopsin: T. P. Sakmar, *Prog. Nucleic Acid Res*. **1998**, *59*, 1 – 34.
[3] R. R. Rando, *Chem. Biol*. **1996**, *3*, 255 – 262.
[4] I. Palings, J. A. Pardoen, E. van den Berg, C. Winkel, J. Lugtenburg, R. A. Mathies, *Biochemistry* **1987**, *26*, 2544 – 2556.
[5] K. Marr, K. S. Peters, *Biochemistry* **1991**, *30*, 1254 – 1258.
[6] A. A. Lamola, T. Yamane, A. Zipp, *Biochemistry* **1974**, *13*, 738 – 745.
[7] B. Borhan, M. L. Souto, H. Imai, Y. Shichida, K. Nakanishi, *Science* **2000**, *288*, 2209 – 2212.
[8] Y. J. Ohkita, J. Sasaki, A. Maeda, T. Yoshizawa, M. Groesbeek, P. Verdegem, J. Lugtenburg, *Biophys. Chem*. **1995**, *56*, 71 – 78.
[9] X. Feng, P. J. E. Verdegem, M. Eden, D. Sandstrom, Y. K. Lee, P. H. M. Bovee-Geurts, W. J. de Grip, J. Lugtenburg, H. J. M. de Groot, M. H. Levit, *J. Biomol. NMR* **2000**, *16*, 1 – 8.
[10] Y. Shichida, F. Tokunaga, T. Yoshizawa, *Biochim. Biophys. Acta* **1978**, *504*, 413 – 430.
[11] A. S. Waggoner, L. Stryer, *Biochemistry* **1971**, *10*, 3250 – 3254.
[12] D. Pan, R. A. Mathies, *Biochemistry* **2001**, *40*, 7929 – 7936.
[13] M. Ishiguro, T. Hirano, Y. Oyama, *ChemBioChem* **2003**, *4*, 228 – 231.
[14] T. Hirano, I. T. Lim, D. M. Kim, X.-G. Zheng, K. Yoshihara, Y. Oyama, H. Imai, Y. Shichida, M. Ishiguro, *Photochem. Photobiol*. **2002**, *76*, 606 – 615.
[15] D. L. Farrens, C. Altenbach, K. Yang, W. L. Hubbell, H. G. Khorana, *Science* **1996**, *274*, 768 – 770.
[16] S. P. Sheikh, T. A. Zvyaga, O. Lichtage, T. P. Sakmar, H. R. Bourne, *Nature* **1996**, *383*, 347 – 350.
[17] P. Ghanouni, J. J. Steenhuis, D. L. Farrens, B. K. Kobilka, *Proc. Natl. Acad. Sci. USA* **2002**, *98*, 5997 – 6002.
[18] C. Longstaff, R. D. Calhoon, R. R. Rando, *Proc. Natl. Acad. Sci. USA* **1986**, *83*, 4209 – 4213.
[19] S. Arnis, K. P. Hofmann, *Proc. Natl. Acad. Sci. USA* **1993**, *90*, 7849 – 7853.
[20] K. Fahmy, T. P. Sakmar, F. Siebert, *Biochemistry* **2000**, *39*, 10607 – 10612.
[21] G. Choi, J. Landin, J. F. Galan, R. R. Birge, A. D. Albert, P. L. Yeagle, *Biochemistry* **2002**, *41*, 7318 – 7324.
[22] T. E. Thorgeirsson, J. W. Lewis, S. E. Wallace-Williams, D. S. Kliger, *Biochemistry* **1993**, *32*, 13861 – 13872.
[23] S. Tachibanaki, H. Imai, T. Mizukami, T. Okada, Y. Imamoto, T. Matsuda, Y. Fukada, A. Terakita, Y. Shichida, *Biochemistry* **1997**, *36*, 14173 – 14180.
[24] S. Tachibanaki, H. Imai, A. Terakita, Y. Shichida, *FEBS Lett*. **1998**, *425*, 126 – 130.
[25] K. Palczewski, T. Kumasaka, T. Hori, C. A. Behnke, H. Motoshima, B. A. Fox, I. Le Trong, D. C. Teller, T. Okada, R. E. Stenkamp, M. Yamamoto, M. Miyano, *Science* **2000**, *289*, 739 – 745.
[26] D. C. Teller, T. Okada, C. A. Behnke, K. Palczewski, R. E. Stenkamp, *Biochemistry* **2001**, *40*, 7761 – 7772.
[27] T. Okada, Y. Fujiyoshi, M. Silow, J. Navarro, E. M. Landau, Y. Shichida, *Proc. Natl. Acad. Sci. USA* **2002**, *96*, 4898 – 4903.
[28] R. S. H. Liu, *Account Chem. Res*. **2000**, *34*, 555 – 562.
[29] U. M. Ganter, W. Gartner, F. Siebert, *Biochemistry* **1988**, *27*, 7480 – 7488.
[30] M. Ishiguro, *J. Am. Chem. Soc*. **2000**, *122*, 444 – 451.
[31] V. Buß, K. Kolster, F. Terstegen, R. Vahrenhorst, *Angew. Chem.* **1998**, *110*, 1997 – 2000; *Angew. Chem. Int. Ed*. **1998**, *37*, 1893 – 1895.
[32] Y. Fujimoto, J. Ishihara, S. Maki, N. Fujioka, T. Wang, T. Furuta, N. Fishkin, B. Boehan, N. Berova, K. Nakanishi, *Chem. Eur. J.* **2001**, *7*, 4198 – 4204.
[33] J. W. Lewis, G.-B. Fan, M. Sheves, I. Szundi, D. S. Kliger, *J. Am. Chem. Soc*. **2001**, *123*, 10024 – 10029.
[34] S. Nishimura, J. Sasaki, H. Kandori, J. Lugtenburg, A. Maeda, *Biochemistry* **1995**, *34* ,16758 – 16763.
[35] T. A. Nakayama, H. G. Khorana, *J. Biol. Chem*. **1991**, *266*, 4269 – 4275.
[36] U. M. Ganter, E. D. Schmid, D. Perez-Sala, R. R. Rando, F. Siebert, *Biochemistry* **1989**, *28*, 5954 – 5962.
[37] M. Beck, T. P. Sakmar, F. Siebert, *Biochemistry* **1998**, *37*, 7630 – 7639.
[38] The previously reported lumirhodopsin model[13] has a right-twisted conformation of the chromophore as well as the polyene plane parallel to the membrane plane. TM3 and TM4 are also in an arrangement similar to that of the present metarhodopsin I model. Thus, the chromophore structure of the previous model is closer to that of the present model of metarhodopsin I. Since the cyclohexenyl group in the present models of lumirhodopsin and metarhodopsin I is located proximal to Cys167 on TM4, the cyclohexenyl group modified for the photoaffinity-labeling experiments[7] would induce deformation at the portion kinked by Pro170 and Pro171 on TM4.
[39] J. F. Resek, Z. T. Farabakhsh, W. L. Hubell, H. G. Khorana, *Biochemistry* **1993**, *32*, 12025 – 12032.
[40] H. Imai, T. Mizukami, Y. Imamoto, Y. Shichida, *Biochemistry* **1994**, *33*, 14351 – 14358.
[41] M. Han, M. Groesbeek, T. P. Sakmar, S. O. Smith, *Proc. Natl. Acad. Sci. USA* **1997**, *94*, 13442 – 13447.
[42] J. Saam, E. Tajkhorshid, S. Hayashi, K. Shulten, *Biophys. J*. **2002**, *83*, 3097 – 3112.

[43] S. Filipek, R. E. Stenkamp, D. C. Teller, K. Palczewski, *Annu. Rev. Physiol.* **2003**, *65*, 851 – 879.
[44] T. Okada, O. P. Ernst, K. Palczewski, K. P. Hofmann, *Trends Biochem. Sci.* **2001**, *26*, 318 – 324.
[45] I. Remy, I. A. Wilson, S. W. Michnick, *Science* **1999**, *283*, 990 – 993.
[46] P. R. Robinson, G. B. Cohen, E. A. Zhukovsky, D. D. Oprian, *Neuron* **1992**, *9*, 719 – 725.
[47] G. B. Cohen, D. D. Oprian, P. R. Robinson, *Biochemistry* **1992**, *31*, 12592 – 12601.
[48] T. P. Sakmar, R. R. Franke, H. G. Khorana, *Proc. Natl. Acad. Sci. USA* **1989**, *86*, 8309 – 8313.
[49] Z. T. Farahbakhsh, K. D. Ridge, H. G. Khorana, W. L. Hubbell, *Biochemistry* **1995**, *34*, 8812 – 8819.
[50] J.-M. Kim, C. Altenbach, R. L. Thurmord, H. G. Khorana, W. L. Hubell, *Proc. Natl. Acad. Sci. USA* **1997**, *94*, 14273 – 14278.
[51] C. Altenbach, K. Yang, D. L. Farrens, Z. T. Farahbakhsh, H. G. Khorana, W. L. Hubbell, *Biochemistry* **1996**, *35*, 12470 – 12478.
[52] C. Altenbach, K. Cai, J. Klein-Seetharaman, H. G. Khorana, W. L. Hubbell, *Biochemistry* **2001**, *40*, 15483 – 15492.
[53] C. Altenbach, J. Klein-Seetharaman, K. Cai, H. G. Khorana, W. L. Hubbell, *Biochemistry* **2001**, *40*, 15493 – 15500.
[54] C. Altenbach, J. Klein-Seetharaman, J. Hwa, H. G. Khorana, W. L. Hubbell, *Biochemistry* **1999**, *38*, 7945 – 7949.
[55] N. G. Abdulaev, K. D. Ridge, *Proc. Natl. Acad. Sci. USA* **1998**, *95*, 12854 – 12859.
[56] J. H. McDowell, T. P. Williams, *Vision Res.* **1976**, *16*, 643 – 646.
[57] C. D. Strader, T. M. Fong, M. R. Tota, D. Underwood, *Annu. Rev. Biochem.* **1994**, *63*, 101 – 132.
[58] F. Heitz, J. A. Holzwarth, J.-P. Gies, R. M. Pruss, S. Trumpp-Kallmeyer, M. F. Hibert, C. Guenet, *Eur. J. Pharmacol.* **1999**, *380*, 183 – 195.
[59] S. Trumpp-Kallmeyer, J. Hoflack, A. Bruinvels, M. Hibert, *J. Med. Chem.* **1992**, *35*, 3448 – 3462.
[60] V. I. Gordeliy, J. Labahn, R. Moukhametzianov, R. Efremov, J. Granzin, R. Schlesinger, G. Buldt, T. Savopol, A. J. Scheidig, J. P. Klare, M. Engelhard, *Nature* **2002**, *419*, 484 – 487.
[61] S. Subramaniam, M. Gerstein, D. Oesterhelt, R. Henderson, *EMBO J.* **1993**, *12*, 1 – 8.
[62] K. Cai, J. Klein-Seetharaman, J. Hwa, W. L. Hubbell, H. G. Khorana, *Biochemistry* **1999**, *38*, 12893 – 12898.
[63] S. W. Lin, T. P. Sakmar, *Biochemistry* **1996**, *35*, 11149 – 11159.
[64] H. Imai, D. Kojima, T. Oura, S. Tachibanaki, A. Terakita, Y. Shichida, *Proc. Natl. Acad. Sci. USA*, **1997**, *94*, 2322 – 2326.
[65] M. S. Weiss, U. Abele, J. Weckesser, W. Welfe, E. Schiltz, G. E. Schulz, *Science* **1991**, *254,* 1627 – 1630.
[66] G. N. Prado, L. Taulor, P. Polger, *J. Biol. Chem.* **1997**, *272*, 14638 – 14642.
[67] S. Acharya, S. S. Karnik, *J. Biol. Chem.* **1996**, *271*, 25406 – 25411.
[68] The coordinates of the intermediate models are available upon request.

Received: May 20, 2003
Revised: October 24, 2003 [F668]

